K.Ouari[1,*]
T.Rekioua[1]
M.Ouhrouche[2]

J. Electrical Systems 9-2 (2013): 243-255

Regular paper

Nonlinear Model Predictive Controller of a variable speed wind turbine driven Doubly Fed Induction Generator

In order to make a wind power generation truly cost-effective and reliable, an advanced control techniques must be used. In this paper, we develop a new control strategy, using nonlinear model predictive control (NMPC) approach, for DFIG-based wind turbine. The DFIG is fed through the rotor windings by a back-to-back converter controlled by Pulse Width Modulation (PWM), where the stator winding is directly connected to the grid. The proposed control law is based on two points: NMPC-based torque-current control loop generating the rotor reference voltage and NMPC-based speed control loop that provides the torque reference. Finally, a real-time simulation is carried out to illustrate the performance of the proposed controller.

Keywords: Nonlinear model predictive control, DFIG-based wind turbine, real-time simulation.

1. Introduction

Recently, many new wind farms have employed wind turbines based on doubly-fed induction generator (DFIG) [1]. Due to their full power control capability, variable speed operation, low converter cost and reduced power loss [2-3]. However, DFIG constitutes a challenging control problem, because of its fast dynamics, and being highly coupled and nonlinear multi-variable system.

The Field-oriented vector control using cascaded PI controllers is widely used, in DFIG-based wind turbines, for reasons of simplicity and applicability [4]. However, PI-type control methods are not effective when the system to be controlled is characterized by strong nonlinearity and external disturbances. To overcome these drawbacks, various approaches have been proposed to replace PI-type controllers. Some examples are the H∞ control theory, neural networks and sliding mode control [5-7].

On the other hand, nonlinear model predictive control (NMPC) refers to a class of computer control algorithms that utilize an explicit process model to predict the future response of a plant. Due to its good robustness for external disturbances and varying parameters, it has received a great deal of attention and is considered by many to be one of the most promising methods in control engineering [8-9].

In this paper, a nonlinear model predictive control (NMPC) is applied to a wind energy conversion system based on Doubly-fed Induction Generator (DFIG). The control law is derived by optimization of an objective function that considers the control effort and the difference between the predicted outputs and their references. The Taylor series expansion is used to approximate the predicted outputs in a finite horizon.

Corresponding author: REKIOUA Toufik, Laboratory of LTII Department of electrical engineering, University of Bejaia, Algeria, E-mail: to_reki@yahoo.fr

[1] LT2I Lab Department of Electrical Engineering, University of Bejaia, Algeria

[2] EMIC Lab, Department of Applied Sciences, University of Quebec at Chicoutimi, Chicoutimi, QC, Canada

The rest of the paper is organized as follows: In section 3, the dynamic model of wind energy conversion system is exposed. In section 4, mathematical formulation of NMPC for nonlinear system is presented. The control system is developed is section 5. The real time simulation results are given in sections 6. Finally, Section 7 concludes the paper.

2. Notation

P_t	Aerodynamic power (W)
ρ_a , v	Air density kg m^3, wind speed
R	Rotor turbine radius (m)
C_p , $C_{p\text{-}max}$	Power coefficient, Maximal power coefficient
β	Blades pitch angle
λ , λ_{opt}	Tip-speed ratio , Optimal tip-speed ratio
T_t , T_r	Aerodynamic torque (N.M), Generator torque (N.m)
Ω_t , Ω_r , $\Omega_{r\text{-}ref}$	Turbine speed , Generator speed, Reference generator speed(rad/s)
G	Gear ratio
$P_{grid\text{-}ref}$	Reference grid active power (W)
η	System (wind turbine + DFIG) efficiency.
P_s, Q_s	Active and reactive stator power (W,var)
P_r, Q_r	Active and reactive rotor power (W,var)
P_f, Q_f	Active and reactive power exchanged between the filter and the grid (W,var)
T_{em}	Electromagnetic torque (N.m)
V_{dr}, V_{qr}	Two-phase rotor voltages (v)
V	Stator voltages (v)
I_{dr}, I_{qr}	Two-phase rotor current (A)
R_r , L_r	Per-phase rotor resistance and self inductance
M, P	Mutual inductance, Number of pole pairs
J, f_r	Moment of inertia , coefficient of friction.
ω_s, ω_r	Stator and rotor angular velocities rd/s
s, σ	*G*enerator *s*lip and Dispersion ratio
x , u , T_r	State vector , Control output, Disturbance
$\mathfrak{J}$	Finite horizon cost function
T_p , ρ_i	Predictive time, Relative degree of the output i
$L_f^k h_i$	The k^{th} order Lie derivative of h_i
R_f X_f	Filter resistance and reactance
PI	Proportional, integral
MPPT	Maximum power point tracking
GST , RST	Grid side converter, Rotor side converter
PWM	Pulse Width Modulation
WECS	wind energy conversion system

3. Modeling of the wind generation system

The system considered in this work is shown in Figure 1. The wind turbine is coupled to the DFIG rotor shaft through a gearbox. The stator windings of DFIGs are directly connected to the grid, and rotor windings are connected to the grid through back-to-back power electronic converters. Between the two converters a dc-link capacitor is placed.

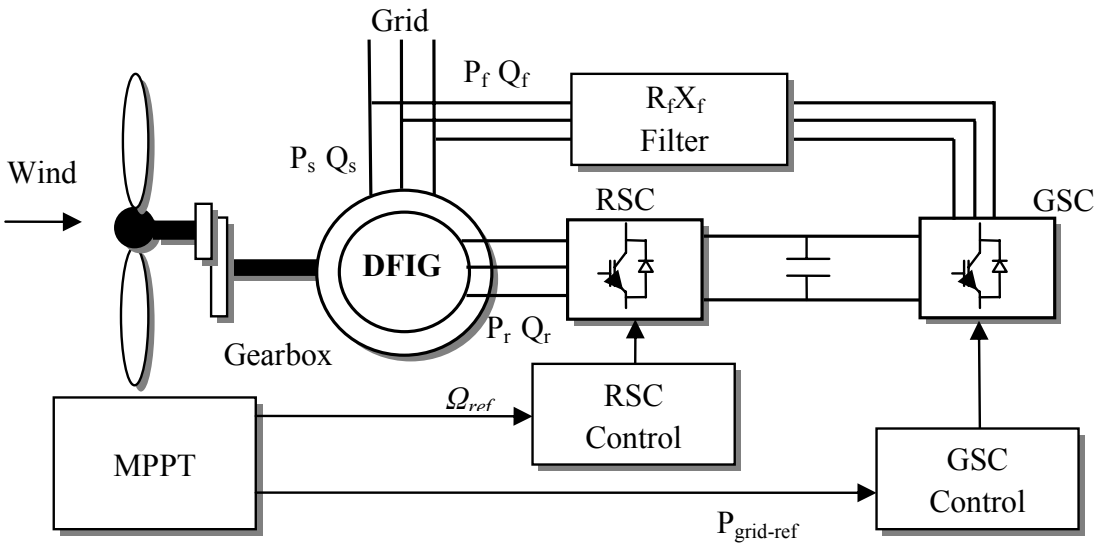

Fig 1: System configuration

3.1 Modeling of the Wind Turbine

The aerodynamic power extracted from the wind can be expressed as

$$P_t = \frac{1}{2}\rho_a \pi R^2 C_p(\lambda,\beta)v^3 \tag{1}$$

The coefficient C_p is specific for each wind turbine. The tip speed ratio is defined as

$$\lambda = \frac{\Omega_t R}{v} \tag{2}$$

A typical relationship between C_p and λ is shown in Figure 2. At the point λ_{opt}, $C_p = C_{p\text{-}max}$, the maximum power can be extracted. To this end, the turbine should always operate at λ_{opt}.

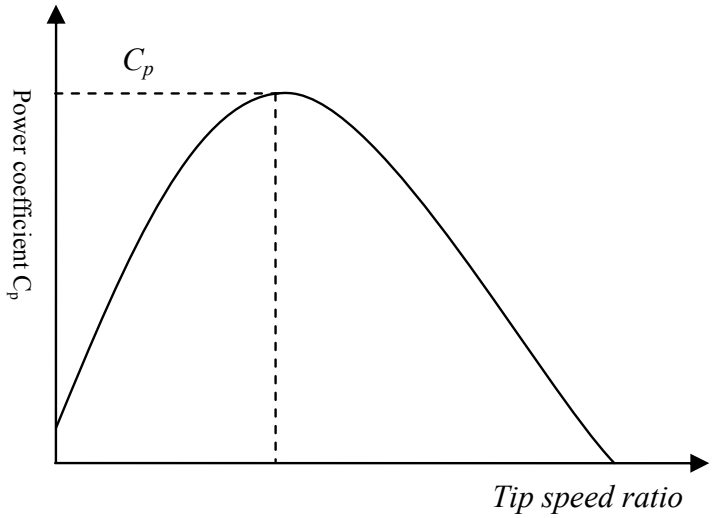

Fig 2: Typical power coefficient.

Neglecting the transmission losses, the torque and speed of the wind turbine, referred to the generator side of the gearbox, are given by

$$T_r = \frac{T_t}{G} \quad , \quad \Omega_t = \frac{\Omega_r}{G} \tag{3}$$

Substituting equation (3) in equations (1) and (2), the rotor speed and active grid power references are given by

$$\begin{cases} \Omega_{r-ref} = \dfrac{\lambda_{opt} G}{R} v \\ P_{grid-ref} = \dfrac{1}{2} \eta \rho_a \pi^2 C_{p-max} v^3 \end{cases} \tag{4}$$

3.2 DFIG model

By choosing a d-q reference frame synchronized with the stator flux, by setting the quadratic component of the stator flux to the null value and by neglecting the stator resistance, the electrical equation of the DFIG is written as follows [10-11]

$$\begin{cases} \dfrac{dI_{dr}}{dt} = -\dfrac{R_r}{\sigma L_r} I_{dr} + s\omega_s I_{qr} + \dfrac{1}{\sigma L_r} V_{dr} \\ \dfrac{dI_{qr}}{dt} = -\dfrac{R_r}{\sigma L_r} I_{qr} - s\omega_s I_{dr} + s\dfrac{MV_s}{\sigma L_r L_s} + \dfrac{1}{\sigma L_r} V_{qr} \end{cases} \tag{5}$$

The electrical model is completed by the mechanical equation given below

$$J\frac{d}{dt}\Omega_r = T_{em} - T_r - f_r\Omega_r \tag{6}$$

The electromagnetic torque generated by the DFIG is given by

$$T_{em} = P\frac{MV_s}{\omega_s L_s} I_{qr} \tag{7}$$

The active and reactive powers exchanged between the stator and the grid can be expressed as follows

$$\begin{cases} P_S = -\dfrac{MV_S}{L_s} I_{qr} \\ Q_S = \dfrac{V_s^{\,2}}{\omega_s L_s} - \dfrac{MV_s}{L_s} I_{dr} \end{cases} \tag{8}$$

with: $\sigma = 1 - \dfrac{M}{L_r L_s}$; $s = \dfrac{\omega_s - \omega_r}{\omega_s}$

4. Mathematical formulation of NMPC

The nonlinear model predictive control proposed by Chen *et al.* [12] is briefly described in this section. The NMPC structure is shown in figure 3.

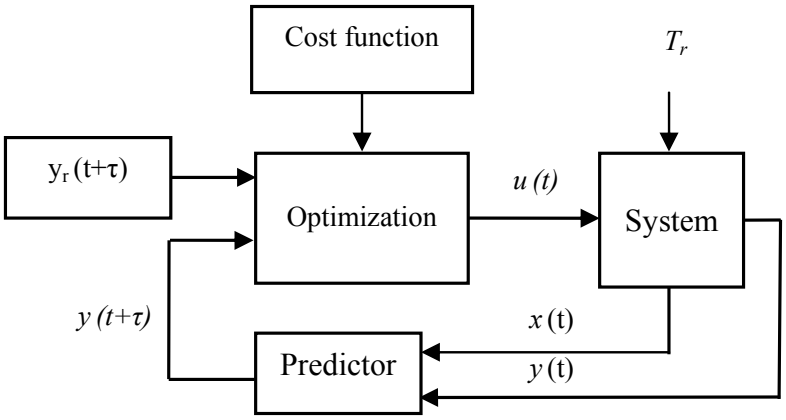

Fig 3: NMPC Structure

We consider a nonlinear system of the form

$$\begin{cases} \dot{x}(t) = f(x) + g_u(x)u(t) + g_T(x)T_r(t) \\ y = h(x) \end{cases} \tag{9}$$

The function $f(x)$ and $h(x)$ are assumed to be continuously differentiable a sufficient number of times. Vector function $g_u(x)$ and $g_T(x)$ are continuous functions of x. The problem consists in elaborating a control law $u(t)$ such that the output $y(t+\tau)$ can optimally track a desired reference $y_r(t+\tau)$ in presence of the disturbance T_r. The predictive control will be optimal if the finite horizon cost function $\Im$ is minimized

$$\Im = \frac{1}{2}\int_{0}^{Tp} [y(t+\tau) - y_r(t+\tau)]^T [y(t+\tau) - y_r(t+\tau)]d\tau \tag{10}$$

To solve the nonlinear optimization problem (10), the predicted output $y(t+\tau)$ and the predicted reference $y_r(t+\tau)$ are approximated by Taylor series expansion

$$y_i(t+\tau) = h_i(x) + \sum_{k=1}^{\rho_i} \frac{\tau^k}{k!} L_f^k h_i(x) + \frac{\tau^{\rho i}}{\rho_i!} L_{gu} L_f^{(\rho_i - 1)} h_i(x) u(t) \tag{11}$$

The Lie derivative of function $h_i(x)$ along a vector field $f(x) = (f_1(x) \ldots\ldots f_n(x))$ is denoted by

$$\begin{cases} L_f h_i(x) = \dfrac{\partial h_i(x)}{\partial x} f(x) \\ L_f^k h_i(x) = L_f \left(L_f^{(k-1)} h_i(x) \right) \\ L_{g_u} L_f h_i(x) = \dfrac{\partial L_f h_i(x)}{\partial x} g_u(x) \\ L_{g_T} L_f h_i(x) = \dfrac{\partial L_f h_i(x)}{\partial x} g_T(x) \end{cases} \tag{12}$$

The necessary condition for the optimal control is given by

$$\frac{d\Im}{du} = 0 \tag{13}$$

5. The control system

The rotor speed is controlled by the rotor side converter (RSC), while the power flow is controlled by the grid side converter (GSC).

5.1 Rotor side converter control

As DFIG is characterized by two-time scales modes; i.e. electrical (fast) and mechanical (slow) modes, a cascaded structure is adopted for the design of the RST controller, see

Figure 4. The inner loop is used to regulate the d-axis rotor current and the electromagnetic torque. The outer loop is employed for the speed trajectory tracking.

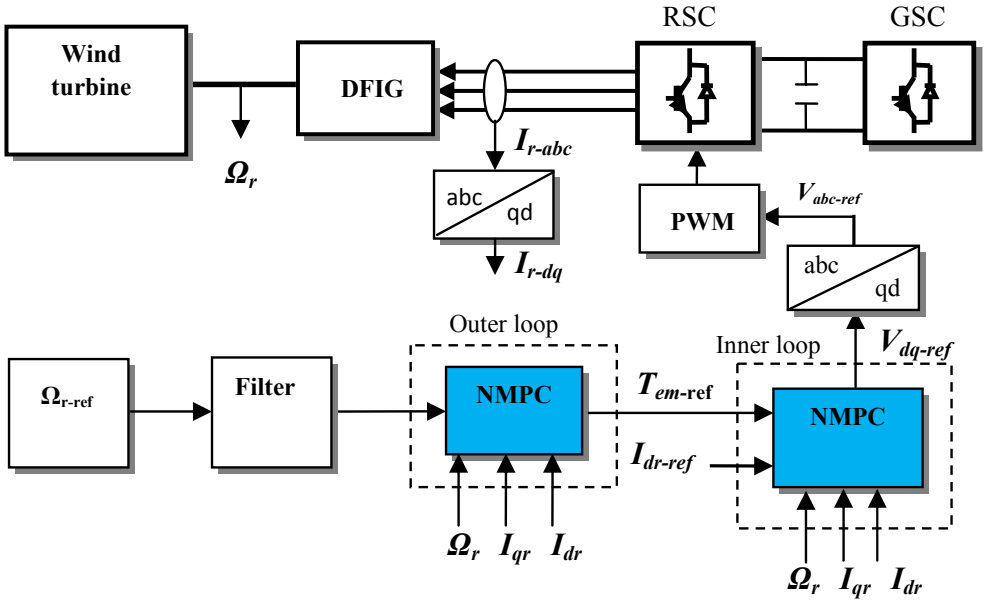

Fig 4: Block Diagram of the proposed NMPC applied to the RSC

5.1.1 Inner control loop

In the internal loop, the predictive control is applied to the electrical equations in order to provide the components of the armature rotor voltage ($V_{d\text{-}ref}$, $V_{qd\text{-}ref}$). From (5), it follows that the electrical equations can be expressed as

$$\begin{cases} \dot{x}(t) = f(x) + g_u(x)u(t) \\ y = h(x) \end{cases} \tag{14}$$

With:

$$x = (I_{dr} \quad I_{qr})^T \quad ; \quad u = (V_{dr-ref} \quad V_{qr-ref})^T \quad ; \quad y = (T_{em} \quad I_{dr})^T$$

The state vector x is composed of the d-axis and q-axis component of the armature rotor currents. The input vector u is made of the d-axis and q-axis components of the armature rotor voltage. The output vector y consists of the electromagnetic torque and the d-axis rotor current, while vector function $f(x)$ and $g_u(x)$ are defined as

$$f(x) = \begin{pmatrix} -\dfrac{R_r}{\sigma L_r} I_{dr} + s\omega_s I_{qr} \\ -\dfrac{R_r}{\sigma L_r} I_{qr} - s\omega_s I_{dr} + s\dfrac{MV_s}{\sigma L_r L_s} \end{pmatrix} ; \quad g_u(x) = \begin{pmatrix} \dfrac{1}{\sigma L_r} & 0 \\ 0 & \dfrac{1}{\sigma L_r} \end{pmatrix}$$

The outputs to be controlled in the inner loop are defined as follows

$$\begin{cases} y_1 = h_1(x) = T_{em} = P\dfrac{MV_s}{\omega_s L_s} I_{qr} \\ y_2 = h_2(x) = I_{dr} \end{cases} \tag{15}$$

For the outputs y_1 and y_2, their relative degrees ρ_1 and ρ_2 are equal to 1. The resulting NMPC applied to the system (14) is given by

$$u(t) = -G_u(x)^{-1}\left[\sum_{i=0}^{1} k_i (L_f^i h(x) - y_r^{[i]}(t))\right] \tag{16}$$

With: $k_0 = \dfrac{3}{2T_{p2}}$; $k_1 = 1$;

$$h(x) = \begin{pmatrix} T_{em} \\ I_{dr} \end{pmatrix} \quad G_u(x) = \begin{pmatrix} P\dfrac{MV_s}{\omega_s L_s}\dfrac{1}{\sigma L_r} & 0 \\ 0 & \dfrac{1}{\sigma L_r} \end{pmatrix}; \quad y_r = \begin{pmatrix} T_{em-ref} \\ I_{dr-ref} \end{pmatrix}$$

The d-axis rotor current reference is calculated to maintain at null value the stator reactive power flow to the grid.

5.1.2 Outer control loop

The speed controller in the outer loop is obtained by considering the mechanical dynamics of the DFIG. From equation 8, it follows that the mechanical equation can be expressed as

$$\begin{cases} \dot{x}(t) = f(x) + g_u(x)u(t) + g_T(x)T_r(t) \\ y = h(x) \end{cases} \tag{17}$$

Where x and u are, respectively, the rotor speed Ω_r and the electromagnetic torque T_{em}. T_r is the aerodynamic torque and the output y is the rotor speed. The vector function $f(x)$, $g_u(x)$ and $g_T(x)$ are given by

$$f(x) = -\frac{f_r}{J}\Omega_r; \quad g_u(x) = \frac{1}{J}; \quad g_T(x) = -\frac{1}{J}$$

The relative degree ρ of the output y is equal to 1. Then, we shall have the optimal control input as

$$u(t) = -G_u(x)^{-1}\left[\sum_{i=0}^{1} k_i (L_f^i h(x) - y_r^{[i]}(t)) + G_T(x)T_r(t)\right] \tag{18}$$

with: $k_0 = \frac{3}{2T_{p2}}; k_1 = 1;\ h(x) = \Omega_r;\ y_r = \Omega_{r-ref}$

$$G_u(x) = \frac{\partial h(x)}{\partial x} g_u(x) = \frac{1}{J}; \quad G_T(x) = \frac{\partial h(x)}{\partial x} g_T(x) = -\frac{1}{J}$$

The rotor speed reference is given in the equation 4. In order to limit the control effort, the reference speed signal is passed through a second order linear filter given by

$$F(s) = \frac{w_n^2}{s^2 + 2\xi\xi_n s + w_n^2} \tag{19}$$

where $w_n = 5$ $\zeta = 1.2$

5.2 Grid side converter control

The GSC is connected to the electrical grid by an intermediary line characterized by a resistance R_f and a reactance X_f as shown in Figure 5.

In a d-q reference frame related to the network angular speed ω_s equal to the synchronous speed, the electrical voltage equation is given by

$$\begin{cases} \dot{x}(t) = f(x) + g_u(x)u(t) \\ y = h(x) \end{cases} \tag{20}$$

with: $x = (I_{fd} \quad I_{fq})^T$; $u = (V_{md} \quad V_{mq})^T$; $y = (P_f \quad Q_f)^T$

The output vector y consists of the active and reactive power transferred to the grid by the GSC, while vector function $f(x)$ and $g_u(x)$ are defined as

$$f(x) = \begin{pmatrix} -\frac{R_f}{Lf} I_{fd} + \omega_s I_{fq} + \frac{1}{L_f} V_{fd} \\ -\frac{R_f}{Lf} I_{fq} - \omega_s I_{fd} + \frac{1}{L_f} V_{fq} \end{pmatrix}; \quad g_u(x) = \begin{pmatrix} -\frac{1}{L_f} & 0 \\ 0 & -\frac{1}{L_f} \end{pmatrix}$$

The outputs to be controlled are defined as follows

$$\begin{cases} y_1 = P_f = V_{fd} I_{fd} + V_{fq} I_{fq} \\ y_2 = Q_f = V_{fq} I_{fd} - V_{fd} I_{fq} \end{cases} \tag{21}$$

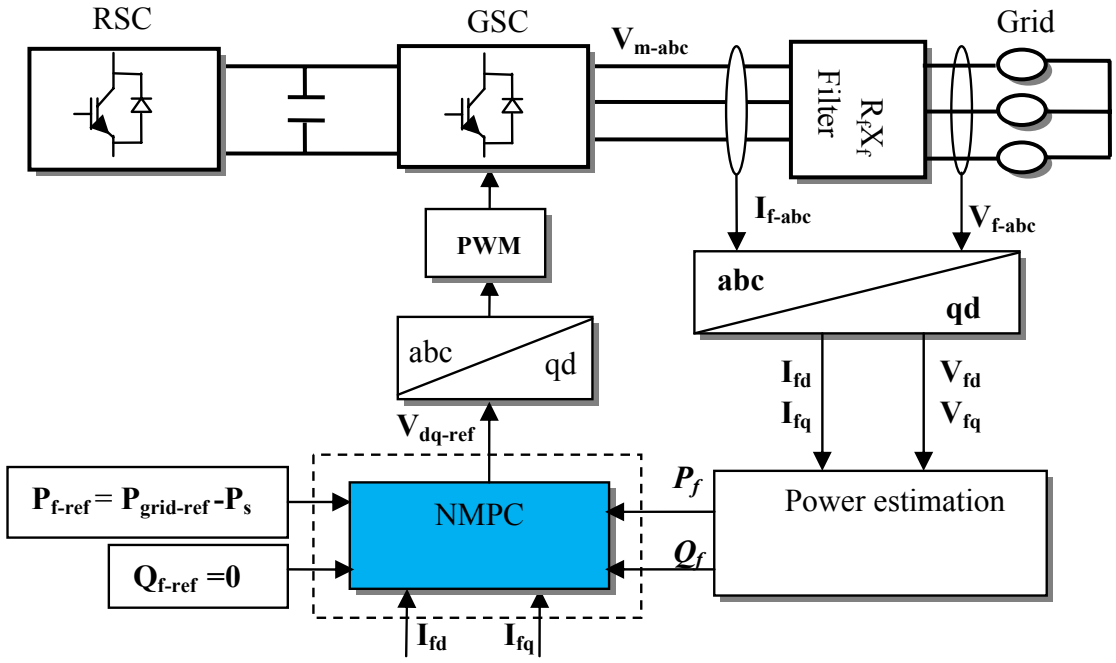

Fig 5: Block Diagram of the proposed NMPC applied to the GSC

The resulting NMPC applied to the system (20) is given by

$$u(t) = -G_u(x)^{-1}\left[\sum_{i=0}^{1} k_i (L_f^i h(x) - y_r^{[i]}(t))\right] \tag{22}$$

with:

$$k_0 = \frac{3}{2T_{p3}}; \quad k_1 = 1; \quad G_u(x) = \begin{pmatrix} -\frac{V_{rd}}{Lf} & -\frac{V_{rq}}{Lf} \\ -\frac{V_{rq}}{Lf} & \frac{V_{rd}}{Lf} \end{pmatrix}; \quad h(x) = \begin{pmatrix} P_f \\ Q_f \end{pmatrix}; \quad y_r = \begin{pmatrix} P_{f-ref} \\ Q_{f-ref} \end{pmatrix}$$

6. Real time simulation results

To evaluate the proposed controller performance, the drive system given in figures 4 and 5 are implemented first in Matlab/Simulink in block diagram format. This Simulink model is then opened and compiled with RT-Lab software package. The predictive time are set to: T_{p1}=0.5ms, T_{p2} = 2ms and T_{p3}=1ms.

6.1 Tracking performance

In this simulation, the robustness of the proposed control law, against the aerodynamic torque variations, is tested. The wind speed profile used in the simulation is illustrated in figure 6. Results of simulation show good tracking capability of the proposed controller.

The speed and electromagnetic torque tracking performances are satisfactory achieved as shown in figures 7 and 8. The stator and rotor active power transited to the grid are plotted in figure 10. We notice that the sense of drainage depends on the sign of the DFIG slip (figure 9). As shown in figure 11, the grid active power tracks perfectly its reference aiming to maximize the conversion efficiency. The rotor and stator reactive powers are shown respectively in figures 12 and 13. The grid reactive power is maintained at zero value contributing to compensate the grid power factor (figure14). The rotor voltage and current at sub-synchronous, synchronous and hyper-synchronous modes are plotted in figure 15.

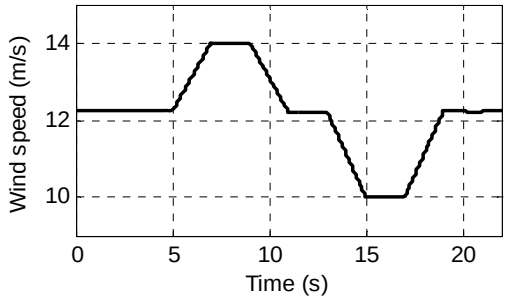

Fig 6: Wind speed profile

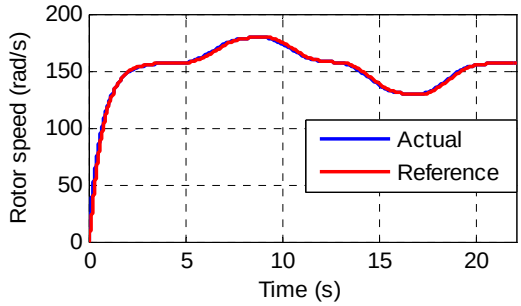

Fig 7: Rotor speed

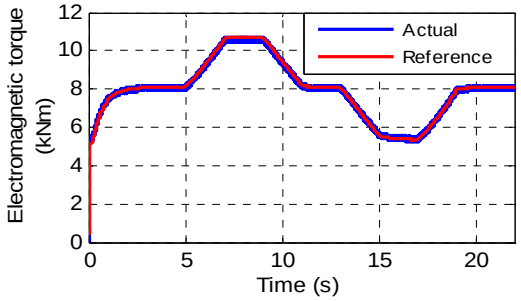

Fig 8: Electromagnetic torque

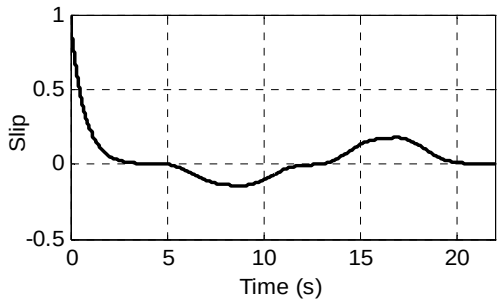

Fig 9: DFIG slip

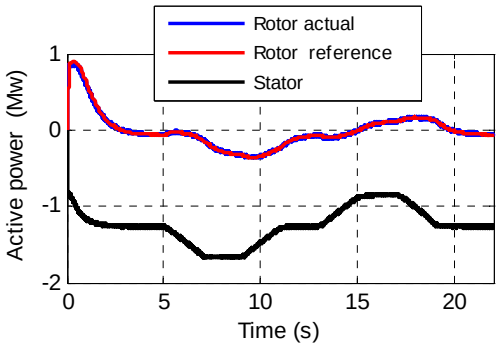

Fig 10: Stator and rotor active power

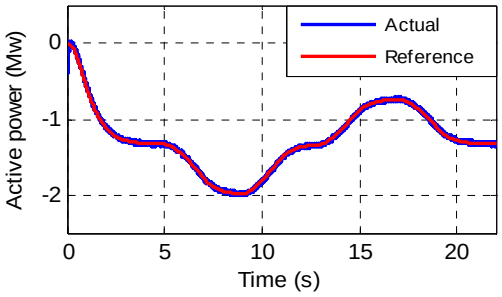

Fig 11: Grid active power

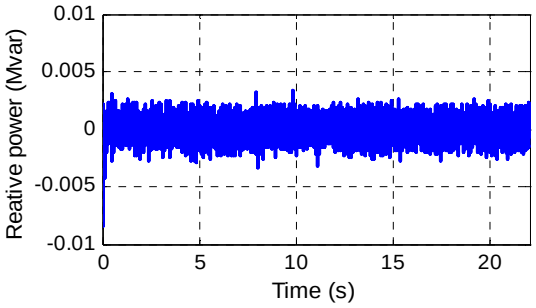

Fig 12: Rotor reactive powers

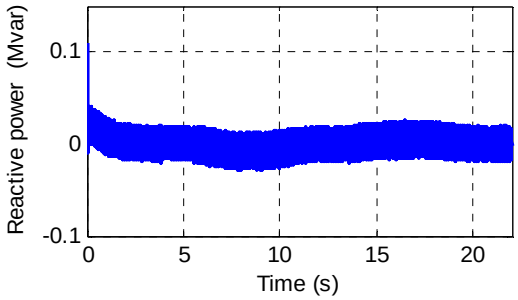

Fig 13: Stator reactive powers.

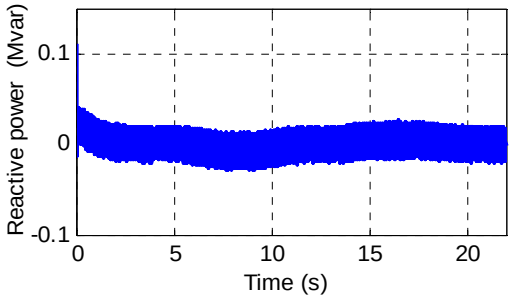

Fig 14: Grid reactive powers

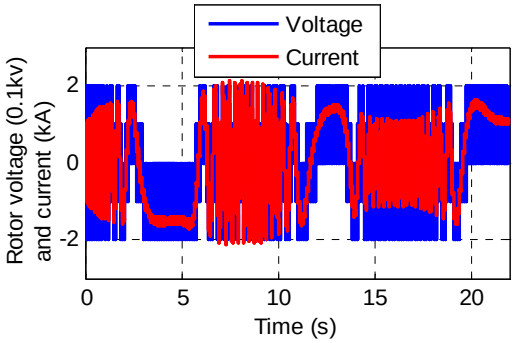

Fig 15: Rotor voltage and current

6.2 Tracking performance under DFIG's parameter variations

As NMPC is a model-based approach, the accuracy of the DFIG parameters may influence the drive. The parameter variations introduced in the DFIG model are set to the following values: 25 % in the rotor resistance at t=4s and 10% in the coefficient of friction at t=16s. These variations are not taken into account in the controller. From Figures 16 and 17, we notice that the systems response convergence to the reference values despite DFIG's parameter variation. Indeed, the grid active power and rotor speed track perfectly their references.

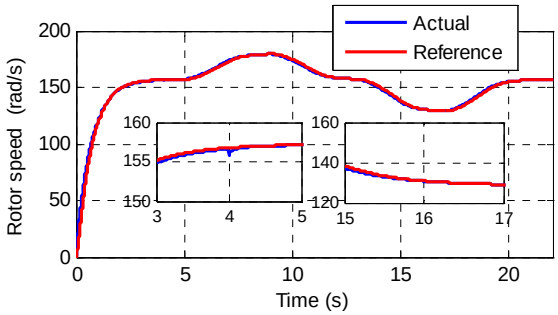

Fig 16: Speed trajectory tracking

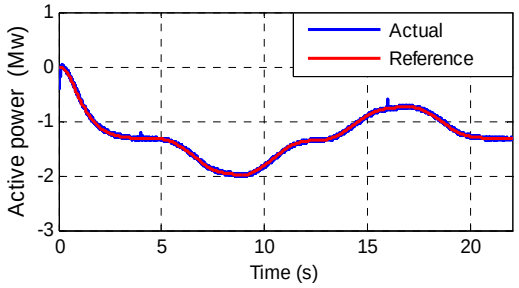

Fig 17: Grid active power under DFIG's parameter variations.

7. Conclusion

In this paper, a NMPC strategy has been proposed for the wind energy conversion system (WECS) based on the DFIG. Simulation results have proven that the proposed controller is able to offer convergence of the system response despite wind speed variations

and DFIG's parameter variations. Indeed, the control strategy achieved a good reference tracking and stability for the rotor speed and electromagnetic torque for the steady state and transient responses of the DFIG. The NMPC strategy is a good candidate for controlling the WECS based on a DFIG interconnected to the grid.

References

[1] Xu. Lie, and Yi. Wang, Dynamic Modeling and Control of DFIG-Based Wind Turbines under Unbalanced Network, Conditions, *IEEE Transaction , On Power systems*, 22(1), 314-323, 2007.
[2] H. Jiabing, N.Heng, X.Hailiang,and H.Yikang, Dynamic Modeling and Improved Control of DFIG Under Distorted Grid Voltage Conditions, *IEEE Trans Energy Conversion*, 26(1), 163-175,2011.
[3] M.Mansour, M.I.Syed, and A.S. Masoum, Impacts of Symmetrical and Asymmetrical Voltage Sags on DFIG-Based Wind Turbines Considering Phase-Angle Jump, Voltage Recovery, and Sag Parameters, *IEEE Power Electron*, 26(526), 1587- 1598, 2011.
[4] H. Jiabing, Direct Active and Reactive Power Regulation of DFIG Using Sliding-Mode Control Approach, *IEEE Trans Energy Conversion*, 25(425), 1028-1039, 2011.
[5] C. Belfedal et al, Robust control of doubly- fed induction generator for stand-alone applications, *Elsevier, Electric Power Systems Research*. .80, 230-239, 2010.
[6] O. Soares, Nonlinear control of the doubly-fed induction generator in wind power systems, *Elsevier, Renewable Energy*, 35, 1662-1670, 2010.
[7] F.Valenciaga, Second order sliding power control for a variable speed-constant frequency energy conversion system, Elsevier, Energy Conversion and Management. 51, pp. 3000-3008,2010.
[8] S.J.Qin, and T.A. Badgwell, A survey of industrial model predictive control technology, *Elsevier Control Eng Practice*, 733-764, 2003.
[9] C.E. Garcia, D.M. Prett, and M. Morari, model predictive control: theory and practice - A survey, *Automatica,* 25(3), 335-348, 1989.
[10] M. Yamamoto, and O. Motoyoshi, Active and reactive power control for doubly-fed wound rotor induction generator, IEEE Transactions on Power Electronics, 6, 624-629, 1991.
[11] B. Hopfensperger, D. Atkinson, and R.A Lakin, Stator-flux-oriented control of a doubly-fed induction machine with and without position encoder, *Inst. Elec. Eng. Proc. Electric Power Applications,* 147(4), 241-250, 2000.
[12] W.H. Chen, D.J. Balance, P.J. Gawthrop, J.J. Gribble, and J. O'Reilly, Nonlinear PID predictive controller, *IEE Proceedings Control Theory application*. 146, 603–611, 1999.

Appendix

1) DFIG: 1.5Mw, 690V, 50Hz, P=2,
$L_s=L_r= 0.0137$ H, $M=0.0135$ H, $R_s= 0.012\ \Omega$,
$R_r = 0.021\ \Omega$, P=2 , $f_r= 0.0071$, $J= 500$ Kg.m^2
2) Wind turbine: Turbine diameter=60m, number of blades=3, hub height=85m, R=36.5m gearbox =90.
3) Filter parameters: $R_f= 1\Omega$ $L_f=30$Mh
4) Dc-link capacitor: $C=500\mu F$, $V_{dc}=400$v